

# Estimating Sea State Using a Low Cost Buoy

Sharon Farber  
 University of Haifa  
 sfarber@univ.haifa.ac.il

Himabindu Allaka  
 University of Haifa  
 himaallaka@gmail.com

Itzik Klein  
 Technion-IIT  
 iklein@technion.ac.il

Morel Groper  
 University of Haifa  
 mgroper@univ.haifa.ac.il

**Abstract**—Wave buoys are widely used to collect ocean data for sea state estimate, several applications such as forecast of weather conditions. To achieve that goal, the industry standard buoys are usually large and expansive as the CAMERI buoy, recently placed at the Haifa bay area. In this paper, we present a newly designed small-size, low-cost autonomous wave buoy equipped with inertial sensors and the ability to log their measurements for offline sea state estimation. A comparison of the estimated sea-state conditions is made between the proposed low-cost compact buoy to the high-end CAMERI buoy using sea experiments conducted at the Haifa bay area. It is shown that a low-cost buoy can serve as a local, short-term deployable data collection unit for various applications.

## I. INTRODUCTION

An ocean wave buoy is an instrument which collects ocean data such as wave height, direction and period ([1], [2]) to represent the sea state. Sea state is the effect that the local winds have on sea conditions, and by that on the vessel's movement. It is usually represented by the maximum wave height, average height of highest one-third waves, average period of waves, and spectral parameters. Unpredictable movement is a major influence factor for the safety, success and overall seaworthiness and cost of an operation.

Usually, the floating buoy has a tethered body equipped with various sensors such as accelerometers, gyroscopes and global positioning system (GPS). Utilizing those different types of sensors allows to estimate basic properties of sea state: sea surface elevation, significant wave height, wave period, dominant wave direction e.t.c. Typically, buoys are equipped with additional sensors to serve as weather buoys collecting temperature, humidity, salinity, depth and current data. This data is used for a variety of applications from predicting weather and earthquakes as well as aiding data during emergency response to chemical spills [3].

Generally, wave buoys are large, expensive and used for long term deployment [3]. They are usually categorized into moored buoys and drifting buoys. Moored buoys are connected with the ocean bottom and take a primary role in measuring sea conditions over the open seas. Drifting buoys are a primary tool used by the oceanographic community to measure local ocean data in high resolution. Commercial directional wave buoys (Eiva, Datawell, Triaxys) can be used as either moored or drift buoys and are built with wave motion sensors based on a stabilized platform including accelerometers, gyroscopes,

magnetic compass and a GPS receiver for monitoring and tracking through HF link telemetry. Equipped with on-board processors and storage, some systems are solar powered while others provide continuous sampling and broadcasting with a battery life of around 1 year and service life of 20 years.

The CAMERI (Datawell Waverider MKIII) buoy is fully autonomous and has high endurance with renewable power source and satellite communication. It is a directional moored wave buoy with a stabilized, gravitationally compensated, platform enabling wave height measurement by a set of three inertial measurement units (IMU) [4] and a GPS. The CAMERI buoy represents the industry standard for accurately measuring heave with a resolution of 1 [cm] within accuracy of < 0.5% (range  $\pm 20[m]$ ) and direction range  $0^\circ - 360^\circ$ , with a resolution of  $1.4^\circ$  and a typical heading error of  $0.5^\circ$ , and has been used extensively for over a decade.

Those characteristics enable high performance yet at same time raise the price of the buoy. Such a high degree of system reliability is not always necessary [5]. As for example, on scientific trials multiple buoys are used as nodes to collect data over a grid or for short term sea state measurements where the buoy is deployed and collected at the end of the experiment.

In this paper, we propose a new design of a low-cost buoy for applications of short term local oceanographic measurements in the Haifa bay area. The proposed buoy has a simple design and small size with a diameter of 1.1[m] and total height of 1[m]. The dimensions were chosen in order to maintain stability at sea while being compact enough to be carried and handled by a single person. Another advantage of such a buoy is the ability to easily deploy and recover from a small vessel, allowing measurement of the sea state in specific zones.

The buoy has an ability to add multiple sensors and serve as a short-term local oceanographic data collection unit. Utilizing that ability, we equipped the buoy with low-cost inertial sensors in order to calculate the sea-state. It is argued that the sea-state estimation accuracy is similar to those calculated by the CAMERI, and thereby enabling the usage of low-cost buoy for estimating sea-state conditions.

The rest of the paper is organized as follows: Section II presents the algorithm used to solve the orientation of the buoy, Section III presents the design of the buoy with low-cost inertial sensors, and the process of calculating the

wave elevation from the acceleration data. Section IV shows the results of the sea experiments and Section V gives the conclusions.

## II. PROBLEM FORMULATION

Magnetic, angular rate, and gravity (MARG) sensor (such as the one used in our low-cost buoy) is an IMU which consist of tri-axis gyroscopes to measure the angular velocity vector, tri-axis accelerometers to measure specific force vector and tri-axis magnetometers to measure the Earth magnetic field. The purpose of the MARG system is to provide the orientation of the buoy relative to a known fixed reference frame. The inertial sensors of the MARG system are subject to misalignment errors and measurements errors including biases and white noise. To mitigate the sensors errors influence on the orientation calculation an orientation filter is used.

The task of the orientation filter is to estimate the buoy orientation through an optimal fusion of gyroscopes, accelerometers and magnetometers measurements. The filter employs a quaternion representation to describe the orientations in 3D and is not subject to the problematic singularities associated with an Euler angle representation. Using the accelerometers and gyroscopes measurements the fusion process is done by calculating the orientation in quaternion form for the measurements.

Section II.A shows the process of estimating the orientation from the angular rate represented using a quaternion vector, Section II.B presents the optimization equations of estimating orientation using gradient descent algorithm for each new sensor measurement, Section II.C expands on the weight functions applied to each orientation calculation and concludes the fusion process.

### A. Estimating Orientation from Angular Rate

An arbitrary orientation of frame E (Earth fixed frame) relative to frame B (Body fixed frame) can be achieved through a rotation of an angle around an axis defined in frame B using a quaternion [6] representation as (eq. 1):

$$\begin{aligned} {}_B \hat{q} &= [q_1 \quad q_2 \quad q_3 \quad q_4] \\ &= [\cos \frac{\theta}{2} \quad -r_x \sin \frac{\theta}{2} \quad -r_y \sin \frac{\theta}{2} \quad -r_z \sin \frac{\theta}{2}] \end{aligned} \quad (1)$$

where,  $q_1$  to  $q_4$  are quaternion components,  $r_x$ ,  $r_y$  and  $r_z$  define the components of the unit vector in the x, y and z and  $\theta$  is the rotation angle around axis  ${}^A \hat{r}$  in frame A as shown in Fig. 1. The mutually orthogonal unit vectors  $[\hat{X}_B, \hat{Y}_B, \hat{Z}_B]$  and  $[\hat{X}_E, \hat{Y}_E, \hat{Z}_E]$  define the principle axis of coordinate frames B and E respectively. A tri-axis gyroscope will measure the angular rate about the x, y and z axes of the body frame B,  $[\omega_x, \omega_y, \omega_z]$  (rad/sec) respectively. The angular rates are written in quaternion vector  $B_\omega$  (eq. 2) by inserting a zero as the first element, the quaternion derivative describing the rate of change of orientation of the earth frame relative to the body frame  ${}_E \dot{q}$  is expressed as in (eq. 3) :

$$B_\omega = [0 \quad \omega_x \quad \omega_y \quad \omega_z]^T \quad (2)$$

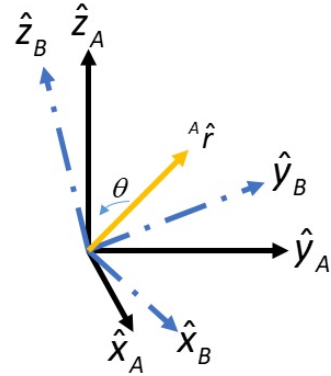


Fig. 1: Orientation of frame B relative to frame A, with angle  $\theta$  around axis  ${}^A \hat{r}$

$${}_E \dot{q} = \frac{1}{2} \cdot {}_E \hat{q} \otimes {}^B \omega \quad (3)$$

The orientation of the E frame relative to the B frame at time t is computed by numerically integrating the quaternion derivative given by (eq. 4) :

$$\begin{aligned} {}_E \dot{q}_{\omega,t} &= \frac{1}{2} \cdot {}_E \hat{q}_{est,t-1} \otimes {}^B \omega_t \\ {}_E q_{\omega,t} &= {}_E \hat{q}_{est,t-1} + {}_E \dot{q}_{\omega,t} \Delta t \end{aligned} \quad (4)$$

Where,  $\Delta t$  is the sampling period and  ${}_E \hat{q}_{est,t-1}$  is the previous estimate of orientation.

### B. Estimating Orientation from Vector Observations

When the direction of an earth's magnetic field is known in the earth frame, a measurement of the field's direction within the sensor frame will allow an orientation of the sensor frame relative to the earth frame to be calculated. However, for any given measurement there will not be a unique sensor orientation solution. A quaternion representation requires a single solution to be found. This may be achieved through the formulation of an optimization problem where the orientation of the sensor,  ${}_E \hat{q}$ , is found by aligning a predefined reference direction of the field in the earth frame,  $\hat{d}_d$ , with the measured field in the sensor (B) frame,  $\hat{d}_s$  by solving (eq. 5):

$$\begin{aligned} \min_{{}_E \hat{q} \in \mathbb{R}} &= f({}_E \hat{q}, {}^E \hat{d}, {}^B \hat{s}) - \text{Objective function} \\ f({}_E \hat{q}, {}^E \hat{d}, {}^B \hat{s}) &= {}_E \hat{q}(\text{conj}) \otimes {}^E \hat{d} \otimes {}_E \hat{q} - {}^B \hat{s} \end{aligned} \quad (5)$$

Where,  ${}_E \hat{q}$  is the orientation of the sensor,  ${}^E \hat{d}$  is the direction of the field in the earth frame, and  ${}^B \hat{s}$  is the direction of the field in the sensor frame.

The following expression (eq. 6) describes the gradient descent algorithm for n iterations resulting in an orientation estimation of  ${}_E \hat{q}_{n+1}$  based on an initial estimated orientation  ${}_E \hat{q}_0$  and a variable step-size  $\mu$ . Next, it computes the error in direction defined by the objective function f, and it's Jacobian J:

$$\begin{aligned} {}_E \hat{q}_{k+1} &= {}_E \hat{q}_k - \mu \frac{\nabla f({}_E \hat{q}_k, {}^E \hat{d}, {}^B \hat{s})}{\| \nabla f({}_E \hat{q}_k, {}^E \hat{d}, {}^B \hat{s}) \|}, k = 0, 1, \dots, n \\ \nabla f({}_E \hat{q}, {}^E \hat{d}, {}^B \hat{s}) &= J^T({}_E \hat{q}, {}^E \hat{d}) f({}_E \hat{q}, {}^E \hat{d}, {}^B \hat{s}) \end{aligned} \quad (6)$$

A conventional approach to optimization would require multiple iterations of (eq. 6) to be computed for each new sensor measurement. However, it is acceptable to compute one iteration per time sample provided that the convergence rate of the estimated orientation governed by  $\mu_t$  is equal or greater than the rate of change of physical orientation. The estimated orientation  ${}^B\hat{q}_{\nabla,t}$  is computed at time t based on a previous estimate of orientation  ${}^B\hat{q}_{est.,t-1}$  and the objective function error  $\nabla f$  defined by sensor measurements sampled at time t, the reader is referred to read the gradient descent algorithm [7] for full development of equations.

### C. Filter Fusion Algorithm

The fusion algorithm purpose is to provide an accurate orientation estimate by filtering out high frequency errors in  ${}^B\hat{q}_{\nabla,t}$  and further use  ${}^B\hat{q}_{\nabla,t}$  to compensate for integral drift in  ${}^B\hat{q}_{\omega,t}$  and provide convergence from initial conditions. The estimated orientation of the earth frame relative to the sensor frame,  ${}^B\hat{q}_{est,t}$ , is obtained through the fusion of the two separate orientation calculations one from gyroscope measurement  ${}^B\hat{q}_{\omega,t}$  and the other from accelerometer measurement  ${}^B\hat{q}_{\nabla,t}$  using the expression (eq. 7) :

$${}^B\hat{q}_{est,t} = {}^B\hat{q}_{\nabla,t} \cdot \gamma_t + (1 - \gamma_t) {}^B\hat{q}_{\omega,t} ; \quad 0 \leq \gamma_t \leq 1 \quad (7)$$

where,  $\gamma_t$  and  $1 - \gamma_t$  are weights applied to each orientation calculation. The fusion process ensures an optimal fusion by assuming that the convergence rate of  ${}^B\hat{q}_{\nabla}$  is equal or greater than the physical rate of change of orientation  ${}^B\hat{q}_{\omega,t}$ .

Fig. 2 presents a block diagram representation of the complete orientation estimation algorithm implementation for an IMU following the scheme developed in [7]. The algorithm calculates the orientation  ${}^B\hat{q}_{est}$  by numerically integrating the estimated rate of change of orientation measured by the gyroscopes  ${}^B\hat{q}_{est}$ . It can be seen from Fig. 2 that first the algorithm estimated orientation  ${}^B\hat{q}_{est}$  from rate of change of orientation measured by the gyroscopes readings  ${}^B\hat{q}_{\omega}$ , with the magnitude of the gyroscope measurement error  $\beta$  removed from the accelerometer measurement.

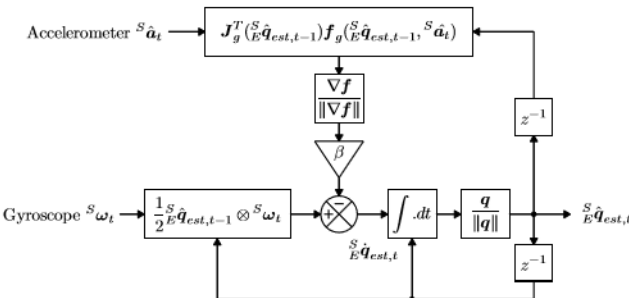


Fig. 2: Fusion algorithm block diagram of the orientation filter

## III. LOW-COST BUOY FOR SEA STATE ESTIMATION

### A. Buoy Design

The Next Generation IMU (NGIMU) is a compact IMU and data acquisition platform that combines on-board sensors and

data processing algorithms [8]. For this purpose the NGIMU sensor was installed inside a watertight enclosure to provide raw data of gyroscopes (range  $\pm 2000^\circ/\text{s}$ , resolution  $0.06^\circ/\text{s}$ ), accelerometers (range  $\pm 16\text{g}$ , resolution  $490\mu\text{g}$ ) and magnetometer (range  $\pm 1300\mu\text{T}$  resolution  $0.3\mu\text{T}$ ) measurements. The sampling frequency of the system is 400 Hz per one 12-bit channel. The water tight enclosure is comprised of several waterproof hulls. The main hull is a cylindrical polyvinyl chloride (PVC) pipe with a set of built-in O-rings, comprising of a second 3D printed acrylonitrile butadiene styrene (ABS) hull specifically designed to outfit the electronics inside. An IP67 box is attached at the top of the PVC pipe to house the GPS, using a cable penetrator between the box and the main hull to provide a waterproof connection between water-tight enclosures. The assembly of the waterproof hulls is inserted inside a discus shaped Styrofoam for flotation (Fig. 3) and a 316 Stainless Steel threaded rod to attach a weight in order to lower the center of mass of the system to increase stability. When deployed, the IMU sensor measurement are logged and stored onto a micro-SD flash memory card using Wi-Fi communication to start and stop a logging session. These sensor measurements are used to calculate the wave elevation data.



Fig. 3: Wave buoy floater

### B. Sea State Calculations

The sea state defining IMU sensor measurements were recorded using the developed wave buoy. The data was filtered in accordance with the work of S.O.H Madgwick [7] in order to estimate the wave elevation.

The sensor data was first processed through an Attitude and Heading Reference Systems (AHRS) algorithm [7] to calculate the orientation of the IMU relative to the Earth. The resultant measurement of acceleration in inertial frame were filtered to remove the bias and misalignment errors. Velocity was calculated by integrating the raw earth acceleration data. The actual velocity data was obtained by removing the drift from the calculated velocity data by performing a high-pass filter on the calculated velocity data. Position data was calculated by integrating the filtered velocity data. The cut-off frequency for the high-pass filter required to remove drift

was identified by performing Fast Fourier Transform (FFT) on the calculated velocity data. The Fourier transformation was done using Matlab FFTW [9] which is a C subroutine library for computing the discrete Fourier transformation (DFT). It is defined for a vector with uniformly sampled points by  $y_{k+1} = \sum_{j=0}^{n-1} \omega^{jk} x_{j+1}; \quad \omega = e^{\frac{2\pi i}{n}}$ . For x and y the indices j and k range from 0 to n-1. The cut-off frequency was selected by the criteria of the mean of data in time domain to be equal to zero. The final position data was obtained by removing the drift from the calculated position data by performing a high-pass filter on the calculated position data. The resultant position data in z-direction is the real-time wave elevation data. The Algorithm is described in the following block diagram (Fig. 4):

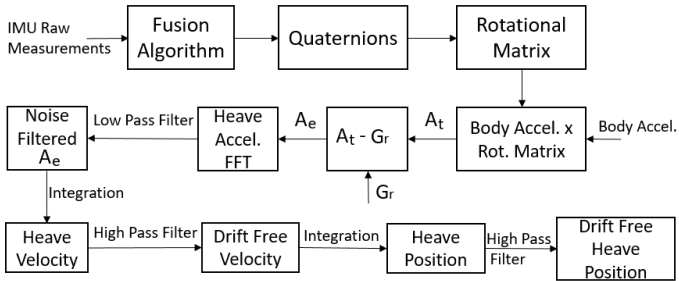


Fig. 4: Top-level block diagram of the system

To compare between the buoy performances, we calculate important parameters that characterize the sea state based on estimated wave elevation data: Maximum wave height  $H_{max}$ , average height of highest one-third waves  $H_{\frac{1}{3}}$ , significant wave height  $H_s$  and period of the spectral peak wave  $T_p$ .

It can be seen in Fig. 5, from the convergence plot that the cumulative  $H_{\frac{1}{3}}$  value converges as the time progresses, where as  $H_{max}$  which is a single event in the total wave record does not converge. Therefore, it was decided to use  $H_{\frac{1}{3}}$  as a comparison criteria between the buoys performance as the measurements have sufficient time and data to converge to a steady value. However  $H_{max}$  values are also presented in this paper.

#### IV. ANALYSIS AND RESULTS

To validate and check the reliability of the self-developed low cost wave buoy, sea experiments were conducted by deploying the low cost wave buoy from a boat approximately 3 [Km] from Haifa bay and next to the CAMERI wave buoy installed in Haifa offshore at coordinates  $32^{\circ}50.63N, 34^{\circ}56.32E$ . The boat used for deploying the low cost wave buoy was sufficiently remote from the experimental zone as not to affect the measurements of the buoy by the wake the boat develops.

The developed low cost wave buoy is equipped with a GPS receiver unit and an IMU which is installed inside a secondary water tight 3D custom printed housing. In regard to the stability of the buoy, the buoy's housing was wrapped inside polystyrene foam disc, 1 [m] in diameter and a 10 [Kg] weight was attached to the buoys housing 0.3 [m] below the

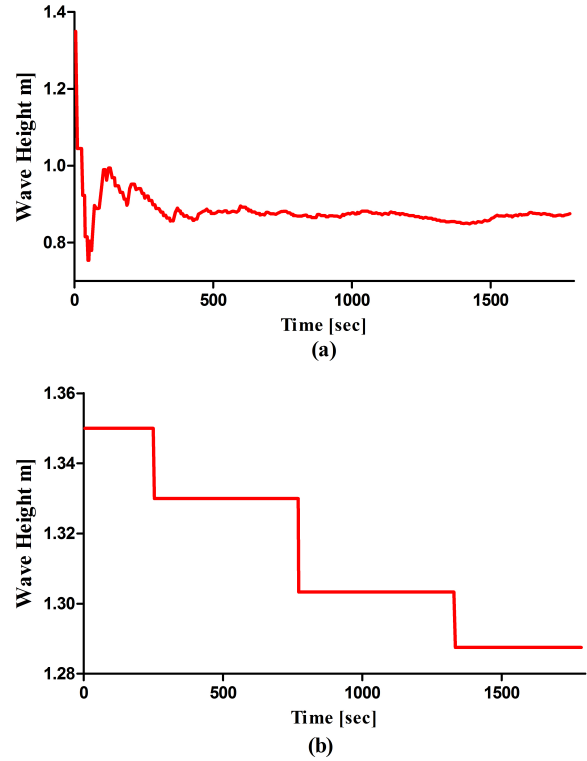


Fig. 5: Wave height convergence plot (a) $H_{\frac{1}{3}}$  and (b)  $H_{max}$

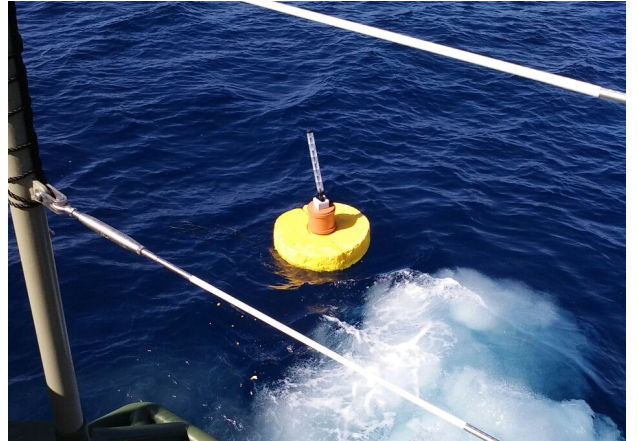


Fig. 6: Wave buoy deployed at sea

water line in order to lower the center of mass of the whole system. Further a reflector was installed on the top of the wave buoy for easy detection and recovery after the experiments.

The real-time wave measurement data from the CAMERI was received in the form of wave elevation measurements, collected at a frequency of 0.78 [Hz]. Similarly, the real-time wave measurement data from the IMU readings (accelerometer, gyroscope and magnetometer) were collected at a frequency of 200 [Hz], using our low cost wave buoy for duration of 120 minutes.

Using the methods described in Section II, IMU measured

data from the low cost wave buoy was processed using Magdwick's gradient descent fusion algorithm to obtain the wave elevation measurements in time domain.

In order to compare our self-devopled wave buoy competence with that of CAMERI wave buoy, The wave elevation data from both buoys were processed to obtain sea state spectral, ( $H_s$ ,  $T_p$ ) and time domain ( $H_m$ ,  $H_{\frac{1}{3}}$ ) parameters for a wave record spanning an interval of 30 minutes each.

In Fig.7 (a) and Fig.7 (b) a comparison of spectral and time domain sea state parameters measured using low cost wave buoy vs CAMERI wave buoy are presented respectively. It is observed from Fig.7 (a) that low cost wave buoy estimated  $H_s$  and  $T_p$  values are withing 5% to that of the CAMERI measurements. Also from Fig.7 (b) it can be observed that low cost wave buoy estimated  $H_{\frac{1}{3}}$  and  $H_{max}$  values are within 15% that of CAMERI estimated values. Considering the fact that  $H_{max}$  value being a singular event for the total wave record, even in this case the comparison is fairly reliable considering an error not exceeding 30%.

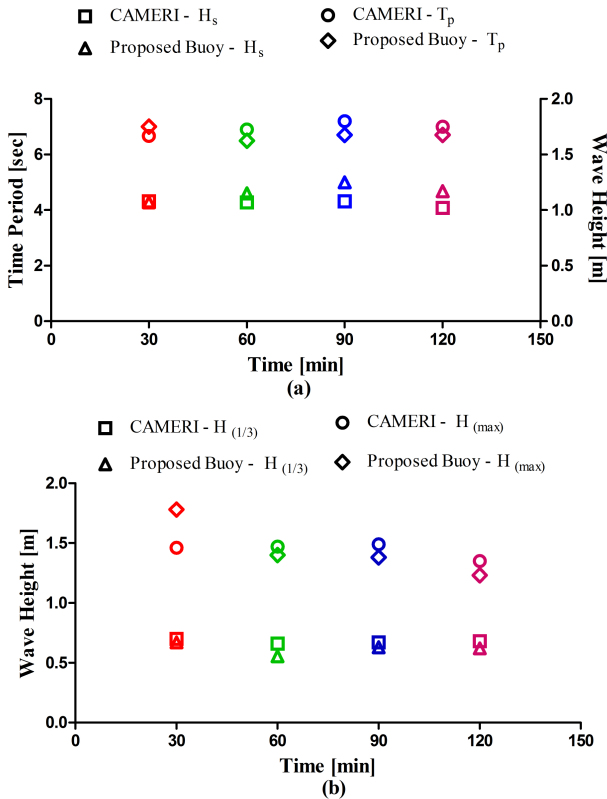


Fig. 7: A comparison between Proposed Buoy and CAMERI wave parameters, (a) spectral and (b) time domain

## V. CONCLUSIONS

A low-cost, small size wave buoy, capable of easy deployment was developed for estimating the sea state. The estimated sea state parameters include: significant wave height, average

height of highest one-third waves, maximum wave height and the period of the spectral peak wave.

To measure the sea state the wave buoy was equipped with necessary inertial and GPS sensors. The results of the proposed low cost buoy estimated sea state parameters from the sea experiments were compared to those obtained from the high-cost CAMERI buoy. It was found that the proposed low-cost buoy estimated sea state parameters are similar to that of the CAMERI buoy.

A major drawback for using low-cost MEMS is their reduced performance at low frequencies due to internal noise. Based on sea trials carried out it was found that such noise can be tolerated as we have found good and consistent measurements for wave parameters.

Furthermore, it was noticed that the difference in between low cost buoy vs CAMERI buoy estimated wave parameters was progressively rising as time progressed, we suspect it could be probably due to the low-cost buoy's drift from the CAMERI buoy during the experiment.

Based on the preliminary sea trials carried out and the degree of accuracy we obtained compared to high-end buoys, we conclude that a small, low-cost buoy equipped with off-the-shelf low cost inertial sensor package can be suitable for use in oceanographic wave measurement.

## REFERENCES

- [1] M. D. Earle and J. M. Bishop, *A practical guide to ocean wave measurement and analysis*. Endeco, 1984.
- [2] M. D. Earle, "Nondirectional and directional wave data analysis procedures," *NDBC Tech. Doc*, vol. 96, no. 002, 1996.
- [3] Y. Hirakawa, T. Takayama, T. Hirayama, and H. Susaki, "Development of mini-buoy for short term measurement of ocean wave," in *OCEANS 2016 MTS/IEEE Monterey*. IEEE, 2016, pp. 1–4.
- [4] Datawell BV, <http://www.datawell.nl/>, Last accessed on 2018-05-21.
- [5] Y. Y. Yurovsky and V. Dulov, "Compact low-cost arduino-based buoy for sea surface wave measurements," in *Progress in Electromagnetics Research Symposium-Fall (PIERS-FALL)*, 2017. IEEE, 2017, pp. 2315–2322.
- [6] J. M. Cooke, M. J. Zyda, D. R. Pratt, and R. B. McGhee, "Npsnet: Flight simulation dynamic modeling using quaternions," *Presence: Teleoperators & Virtual Environments*, vol. 1, no. 4, pp. 404–420, 1992.
- [7] S. O. Magdwick, A. J. Harrison, and R. Vaidyanathan, "Estimation of imu and mag orientation using a gradient descent algorithm," in *Rehabilitation Robotics (ICORR), 2011 IEEE International Conference on*. IEEE, 2011, pp. 1–7.
- [8] Ngimu by x-io Technologies, <http://www.x-io.co.uk/ngimu/>, Last accessed on 2018-05-21.
- [9] M. Frigo and S. G. Johnson, "Fftw: An adaptive software architecture for the fft," in *Acoustics, Speech and Signal Processing, 1998. Proceedings of the 1998 IEEE International Conference on*, vol. 3. IEEE, 1998, pp. 1381–1384.